X-ray diffraction analysis of stannite, wurtz-stannite and pseudo-cubic quaternary compounds by Rietveld method

M. Quintero[a,*], J. Marquina[b], E. Quintero[a], E. Moreno[a], S. Álvarez[a,b], C. Rincón[a], P. Grima[a], P. Bocaranda[a], D. Rivero[a], J. A. Henao[c], and M. A. Macías[c]

[a] *Centro de Estudios de Semiconductores (CES), Departamento de Física, Facultad de Ciencias, Universidad de Los Andes, Mérida 5101, Venezuela.*

[*] *e-mail: mquinterg@gmail.com; mquinter@ula.ve*

[b] *Centro de Estudios Avanzados en Óptica (CEAO), Departamento de Física, Facultad de Ciencias, Universidad de los Andes 5101, Venezuela.*

[c] *Grupo de Investigación en Química Estructural (GIQUE), Facultad de Ciencias, Escuela de Química, Universidad Industrial de Santander, Apartado aéreo 678, Bucaramanga, Colombia.*

Received 6 November 2012; accepted 17 February 2014

Room temperature X-ray powder diffraction measurements were carried out on nine polycrystalline samples of the $Cu_2B^{II}C^{IV}X_4$ (B=Mn, or Fe, or Co; C=Si, or Ge, or Sn; X=S, or Se, or Te) magnetic semiconductor compounds. The diffraction patterns were used to show the equilibrium conditions and to derive crystalline parameter values. The results showed that four of these compounds have a tetragonal stannite structure with space group $I\bar{4}2m$(N° 121), two an orthorhombic wurtz-stannite structure with space group $Pmn2_1$(N° 31) and three of them an orthorhombic pseudo-cubic structure with space group F222 (N° 22). In each case, the structure was refined using the Rietveld method. When the obtained atomic parameter values for the tetragonal compounds were plotted as a function of molecular weight W, it was found that the values of the atomic positions, the cation-anion bond distances, tetragonal distortion and internal distortion of the compounds containing S and/or Se lay on different lines. Also, it was found that when the experimental points of the cation-anion bond distances d_{Cu-VI}, d_{II-VI} and d_{IV-VI} were plotted against the effective lattice parameter $a_e = (V/N)^{1/3}$, a linear variation of these distances with a_e was obtained. Values of the ionic energy gap C_i and homopolar energy gap E_h using the Phillips-Van Vechten scheme, with the present experimental crystallographic results as well as using the atomic data, were determined. It was found that the observed and predicted values of C_i and E_h lie on the same straight line.

Keywords: Magnetic semiconductors; crystal structure; X-ray powder diffraction; Rietveld refinement; crystal growth.

PACS: 61.05.cp; 61.50-f; 61.66.Fn; 75.50Pp

1. Introduction

The magnetic semiconducting quaternary compounds (MSC) of the family I_2-II-IV-VI_4 (I=Cu, Ag; I=Mn, Fe, Co; IV=Si, Ge, Sn; VI=S, Se, Te), which are found in the section $(I_2\text{-}IV)_{1-x}II_{3x}VI_3$ at x = 0.25, are of great interest because of both their applications in the fabrication of low cost solar cells [1] and their large magneto-optical effects which are observed when II are paramagnetic atoms [2-5]. It has been shown that some of the I_2-(Mn,Fe)-IV-VI_4 compounds are antiferromagnetic [2-5]. However, no information on the type of magnetic interaction of the I_2-Co-IV-VI_4 materials has been given so far in the literature, and this will be reported in a further work. Structural studies carried out on some member of this family indicate that they normally crystallize in a sphalerite derivate structure with tetragonal space group $I\bar{4}2m$, or in a wurtzite derivative structure with orthorhombic space group $Pmn2_1$, or in an pseudo-cubic structure with orthorhombic space group F222 [6-9]. The crystal parameter values for the Cu_2MnGeS_4, Cu_2MnSnS_4, Cu_2CoSiS_4, $Cu_2CoSnSe_4$, and $Cu_2CoGeSe_4$ compounds have been determined in Refs. 6, 7, 10. No complete crystal structure determination has been reported for the Cu_2MnSiS_4, Cu_2FeGeS_4, $Cu_2CoSiSe_4$ and $Cu_2CoGeTe_4$ compounds. Hence, in the present work powder X-ray diffraction measurements were carried out on the later compounds, and the results of their crystal structure refinements obtained using the Rietveld method are given. In addition, X-ray powder diffraction measurements and Rietveld studies were also performed on Cu_2MnGeS_4, Cu_2MnSnS_4, Cu_2CoSiS_4, $Cu_2CoSnSe_4$, and $Cu_2CoGeSe_4$, and the obtained results compared with previously reported data.

2. Experimental Details

The samples were prepared using high-purity elements with a nominal purity of at least 99.99 wt%. In each case, the components of 1 g sample were sealed under vacuum ($\approx 10^{-5}$ Torr) in a small quartz ampoule, which had previously been carbonized to prevent interaction of the components with the quartz. The synthesis was realized inside a vertical furnace. The ampoules with the components (1 g sample) were heated up to 200°C and kept for about 1-2 h, then the temperature was raised to 500°C using a rate of 40 K/h, and held at this temperature for 14 h. After, the samples were heated from 500°C to 800°C at a rate of 30 K/h and kept

at this temperature for another 14 h. Then it was raised to 1150°C at 60 K/h, and the components were melted together at this temperature for about 2-3 hours in order to homogenize the material. The furnace temperature was brought slowly (4 K/h) down to 600°C, and the samples were annealed at this temperature for 1 month. Then, the samples were slowly cooled to room temperature using a rate of about 2 K/h.

A small amount of each compound was gently ground in an agate mortar and sieved to a grain size of less than 38 μm. Each sample was mounted on a zero-background specimen holder for the respective measurement. X-ray powder diffraction patterns of the samples were recorded using a D8 FOCUS BRUKER diffractometer operating in Bragg-Brentano geometry equipped with an X-ray tube (Cu Kα radiation: λ = 1.5406 Å, 40 kV and 40 mA) using a nickel filter and an one-dimensional LynxEye detector. A fixed antiscatter slit of 8 mm, receiving slit of 1 mm, soller slits of 2.5° and a detector slit of 3 mm were used. The scan range was from 2 to 70° 2θ with a step size of 0.02° 2θ and a counting time of 0.4 s/step.

3. Results, analysis and Discussions

The crystal structure determination was performed using the DICVOL06 (with an absolute error of 0.03° 2θ), CHECKCELL (used for space group estimation) and NBS*AIDS83 software packages [11-13]. Based on these considerations, a complete crystal structure refinement was performed for each compound using the fitting program MAUD (Material Analysis Using Diffraction) [14] based on Rietveld method [15].

The results of the Rietveld calculation as well as the experimental X-ray conditions used are summarized in Table I. The final atomic positions are given in Table II and the selected cation-anion distance $d_{\text{cation}-\text{anion}}$ and angle values are listed in Table III. As it was expected, the obtained lattice parameter, atomic coordinates and bond distance values for the Cu_2MnSnS_4, Cu_2CoSiS_4, $Cu_2CoSnSe_4$ compounds with stannite structure I$\bar{4}$2m, $Cu_2CoGeSe_4$ with pseudo-cubic orthorhombic structure F222 and Cu_2MnGeS_4 with orthorhombic wurtz-stannite structure Pmn2_1, given in Tables I, II and III, are in good agreement with those reported in earlier works [6,7,10].

Regarding to the Cu_2MnSiS_4, Cu_2FeGeS_4, $Cu_2CoSiSe_4$ and $Cu_2CoGeTe_4$ compounds for which x-ray experimental data are scarcer, it was found that Cu_2FeGeS_4 is tetragonal stannite I$\bar{4}$2m and Cu_2MnSiS_4 is orthorhombic wurtz-stannite Pmn2_1. In the case of the $Cu_2CoSiSe_4$ and $Cu_2CoGeTe_4$ compounds, initially simulate patters were calculated assuming a = b $\approx$ 5.57 Å and c $\approx$ 10.98 Å for I$\bar{4}$2m and/or I$\bar{4}$. But, the experimental patterns could not be explained with these space groups, because of the tetragonal diffraction lines such as (002), (101), (110), (103), (114) were absent. Also, neither double cell along c-axis nor well-defined cubic cell was observed in the experimental diffraction patterns. Moreover, the experimental diffractograms could not be indexed in a hexagonal unit cell. Hence, the X-ray diffraction peaks for the $Cu_2CoSiSe_4$ and $Cu_2CoGeTe_4$ compounds were very well indexed in an orthorhombic face-centered unit cell. The space group F222 was used for the crystal structure determination. The obtained results were similar to those obtained in this work and by Gulay *et al*. [7] for the $Cu_2CoGeSe_4$ compound. It is to be mentioned that for a small unit cell containing only one set of four symmetry-related atomic positions for the metal atoms must induce disorder for these atoms. Because of the very similar scattering powers of the metal atoms involved, the X-ray diffraction lines due the ordering of the cations in the unit cell could not be detected. Hence, it would be possible that the refinement in space group F222 does not provide the correct ordering scheme of the cations, but just results in an average crystal structure. In order to get more insight on this crystal structure, additional techniques are needed, hence, it is planned to carry out Raman spectroscopy and neutron diffraction experiments in a near future.

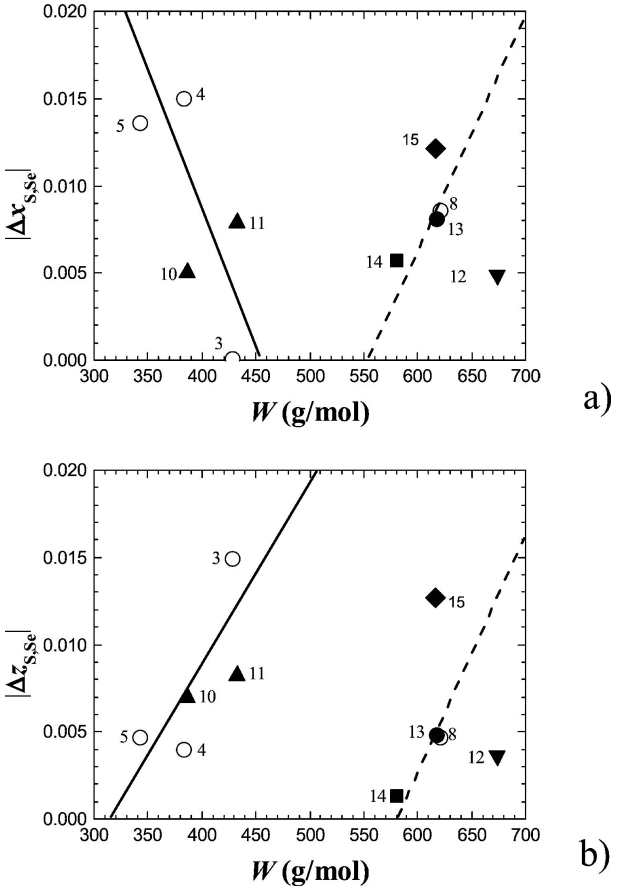

FIGURE 1. (a) Absolute values of anion displacement parameters Δx_S vs W and Δx_{Se} vs W. (b) Absolute values of anion displacement parameters Δz_S vs W and Δz_{Se} vs W. Open circles: present work. Close triangles: Ref. 7. Close upside down triangle: Ref. 18. Close circle: Ref. 16. Close squares: Ref. 17. Close diamond [19]. Solid line: compounds with S. Dashed line: compounds with Se. Materials are labeled in Table IV.

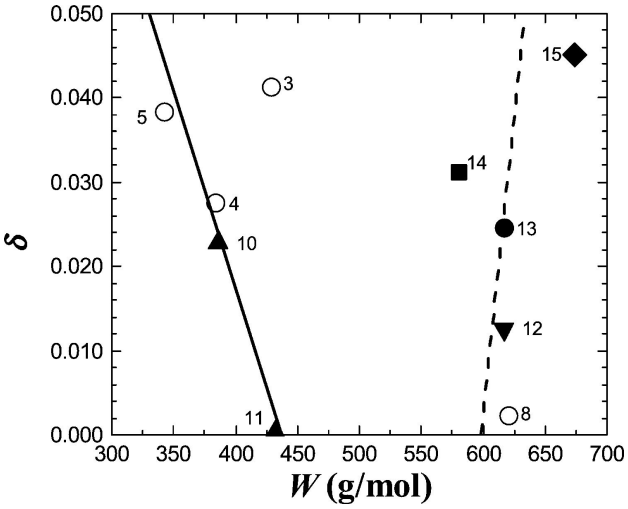

FIGURE 2. Variation of the values of tetragonal distortion δ vs W. Open circles: present work. Close triangles: Ref. 7. Close upside down triangle: Ref. 18. Close circle: Ref. 16. Close squares: Ref. 17. Close diamond [19]. Solid line: compounds with S. Dashed line: compounds with Se. Materials are labeled in Table IV.

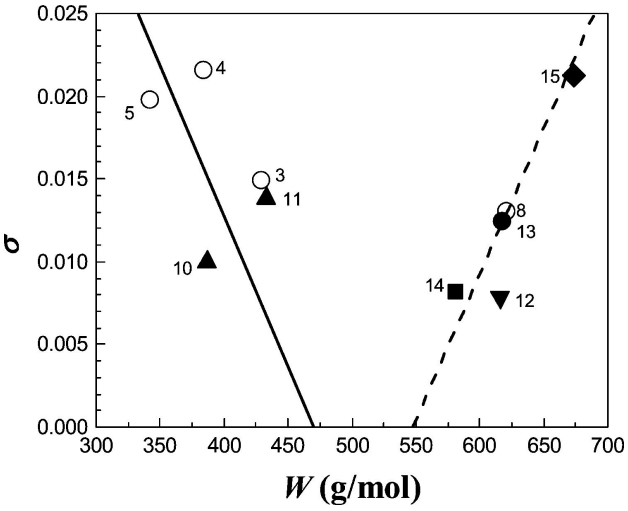

FIGURE 3. Variation of the values of internal distortion σ vs W. Open circles: present work. Close triangles: Ref. 7. Close upside down triangle: Ref. 18. Close circle: Ref. 16. Close squares: Ref. 17. Close diamond [19]. Solid line: compounds with S. Dashed line: compounds with Se. Materials are labeled in Table IV.

In the case of the tetragonal stannite compounds, the absolute values of the anion (S,Se) displacement, from their ideal position, $\Delta x_{S,Se} = \Delta y_{S,Se}$ (=1/4-$x_{S,Se}$) and $\Delta z_{S,Se}$ (=1/8-$z_{S,Se}$) as a function of W are shown, respectively, in figures 1a and 1b.The resulting values of the tetragonal distortion (δ=2-c/a) of the stannite along the [001] direction [16] and the internal distortion

$$\left(\sigma = \Big[(1/4 - x_{S,Se})^2 + (1/4 - y_{S,Se})^2 + (1/8 - z_{S,Se})^2 \Big]^{1/2}\right)$$

[16] as a function of W are shown plotted in Figs. 2 and 3, respectively. The compounds are labeled in the Table IV. It can be seen from figs. 1a and 1b that, within the limits of the experimental errors, the absolute values of Δx_S vs W and Δx_{Se} vs W (in Fig. 1a) as well as Δz_S vs W and Δz_{Se} vs W (in Fig. 1b) lay on different lines. The same behavior is observed from Figs. 2 and 3 for the values of δ and σ respectively, which also lay on different lines. This behavior would be due to the large difference between the atomic weight of the S and Se atoms. Also, it is observed, from Figs. 1a, 1b, 2 and 3 that, for the S compounds, the absolute values of Δx_S, δ and σ decrease with W, while Δz_S increases with W. In the case of the Se compounds, the absolute values of Δx_{Se}, Δz_{Se}, δ and σ increase with W. The decrease of δ and σ with W for the S materials indicates that the tetragonal stannite structure tends toward ideal configurations, *i.e.* $\delta \to 0$ and $\sigma \to 0$. While for the Se materials, the increase of δ and σ with W shows deviations from ideal structural conditions.

It was observed that, in each case, if the resulting experimental values of the cation-anion distances d for the tetragonal and orthorhombic samples, given in Table III, are plotted as a function of W no systematic variation was obtained. However, when these experimental values of d were plotted as a function of the effective lattice parameter $a_e = (V/N)^{1/3}$, where V is the volume of the unit cell and N the number of molecules per cell [10] (N = 2 for $I\bar{4}2m$ or Pmn2$_1$ and N = 1 for F222), it was found that a systematic variation is observed in each case. This is illustrated in figure 4 where it is seen that, within the limits of experimental errors, the values of $d_{\text{Cu - VI}}$, $d_{\text{II - VI}}$ and $d_{\text{IV - VI}}$ increase linearly with the parameter a_e.

Since the present tetrahedrally bonded compounds have semiconducting properties, here, it was of interest to determine values of the ionic energy gap C_i and homopolar energy gap E_h using the Phillips-Van Vechten [20-21] scheme with the present experimental crystallographic results. For the present A_2BCD_4 compounds, the relations for C_i and E_h can be written as [8],

$$1/E_h^2 = 1/3[1/E_h^2(\text{AD}) + 1/E_h^2(BD) + 1/E_h^2(\text{CD})] \quad (1)$$

$$1/Ci^2 = 1/3[1/Ci^2(\text{AD}) + 1/Ci^2(\text{BD}) + 1/Ci^2(\text{CD})] \quad (2)$$

$$E_h(\text{AD}) = ad^{2.5}(\text{AD}) \quad (3)$$

$$E_h(\text{BD}) = ad^{2.5}(\text{BD}) \quad (4)$$

$$E_h(\mathrm{CD}) = ad^{2.5}(\mathrm{CD}) \quad (5)$$

$$C_i(\mathrm{AD}) = 14.4b(Z_A/r_A + Z_D/r_D) \times \exp[k_s(r_A + r_D)/2] \quad (6)$$

$$C_i(\mathrm{BD}) = 14.4b(Z_B/r_B + Z_D/r_D) \times \exp[k_s(r_B + r_D)/2] \quad (7)$$

$$C_i(\mathrm{CD}) = 14.4b(Z_C/r_C + Z_D/r_D) \times \exp[k_s(r_C + r_D)/2] \quad (8)$$

$$f_i = C_i^2/(C_i^2 + E_h^2) \quad (9)$$

k_s is the Thomas-Fermi screening parameter for a tetrahedral bonded crystal with a density of four electrons per site volume given by k_s = 4.86/$(a_e)^{1/2}$ Å^{-1} where a_e is the effective lattice parameter of the compound. Z_A, Z_B, Z_C, Z_D are the valence number of the atoms. The constants a and b are given by a = 40.47 (eV Å)$^{5/2}$ [8] and b = 1.5 [21]. These experimental values can then be compared with the ones obtained without using quaternary compound data. In this case, the various crystallographic parameters are related to the covalent radii r_A, r_B, r_C and r_D of the constituent elements, and the bond length between the concerned ions is given by the sum of the covalent radii of the elements.

Hence, using the experimental data given in table III and the values of the covalent radii of the elements [22], observed and predicted values of C_i and E_h were determined from Eqs. 1 to 9. The resulting observed and predicted plots of C_i vs E_h are shown in Fig. 5. The obtained curves of C_i vs a_e and E_h vs a_e are shown in Fig. 6. It can be seen from

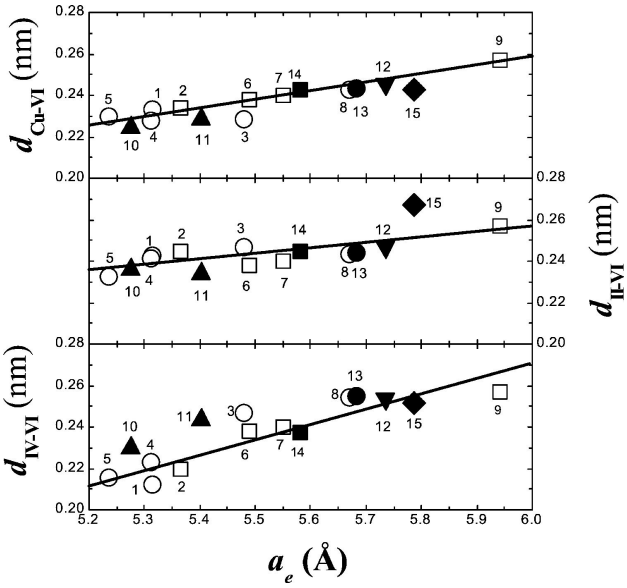

FIGURE 4. Variation of cation-anion distances $d_{\mathrm{Cu-VI}}$, $d_{\mathrm{II-VI}}$ and $d_{\mathrm{IV-VI}}$ as a function of a_e for the compounds indicated in the inset. Open circles present work: tetragonal. Open squares present work: orthorhombic. Close triangles: Ref. 7. Close upside down triangle: Ref. 18. Close circle: Ref. 16. Close squares: Ref. 17. Close diamond [19]. Materials are labeled in Table IV.

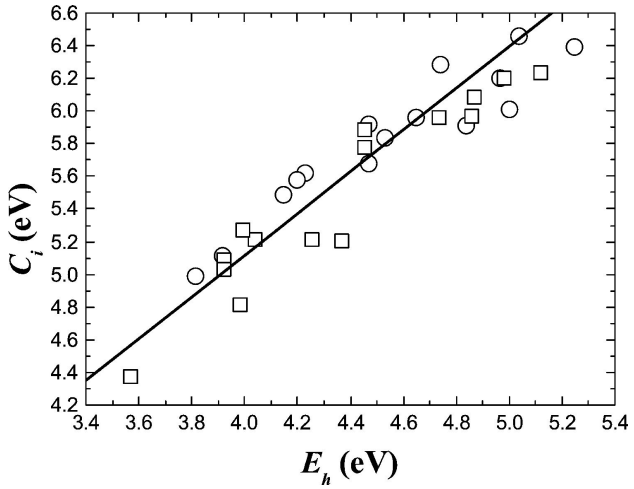

FIGURE 5. Plot of ionic C_i vs homopolar E_h energy gaps. Open circles: obtained values. Open squares: predicted values.

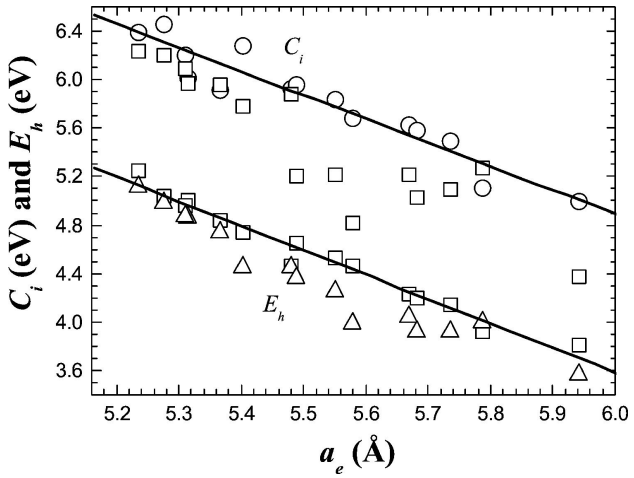

FIGURE 6. Variation of the ionic C_i and homopolar E_h energy gaps as a function of a_e. Open circles: observed *Ci*; close triangles: predicted *Ci*. Close circles: observed E_h; open triangles: predicted E_h.

Fig. 5 that, within the limits of experimental errors, the resulting observed and the predicted values of C_i and/or E_h lie on a same straight line, independently of the crystal structure and kind of anion involved. As it was expected, it appears that all the compounds lie on the four-fold coordination field of the Phillips plot [21], *i.e.* the mean observed iconicity parameter value f_i was found to be about 0.8 times lower than the Phillips iconicity line value (f_i = 0.785). These results are of interest since the values of C_i and E_h, for a quaternary tetrahedrally coordinated crystal with effective lattice parameter a_e, can be very well predicted based only on their constituents atomic properties data. Hence, it would be possible to predict the properties of postulated materials without direct resort to experiment. It is seen from Fig. 6 that the observed values of C_i and E_h decrease linearly with the parameter a_e. These behaviors are consistent with the linear increase of the cation-anion distances with a_e shown in Fig. 4.

TABLE I. Notes: The R_{wp}, R_B, R_{exp} and χ parameters are given in Ref. 16. $^*N$ is the number of formula units per unit cell.

Compound	**Cu_2CoSiS_4**	**Cu_2MnSnS_4**	**Cu_2FeGeS_4**	**$Cu_2CoSnSe_4$**	**$Cu_2CoSiSe_4$**	**Cu_2MnSiS_4**	**$Cu_2CoGeTe_4$**	**Cu_2MnGeS_4**	**$Cu_2CoGeSe_4$**
***N****	2	2	2	2	1	2	1	2	1
Space group	$I\bar{4}2m$	$I\bar{4}2m$	$I\bar{4}2m$	$I\bar{4}2m$	F222	$Pmn2_1$	F222	$Pmn2_1$	F222
***a*(nm)**	0.52693(1)	0.55202(2)	0.53349(1)	0.56711(1)	0.5568(3)	0.75362(9)	0.5966(2)	0.76162(4)	0.56025(1)
***b* (nm)**	0.52693(1)	0.55202(2)	0.53349(1)	0.56711(1)	0.5501(2)	0.64416(4)	0.5922(3)	0.65167(3)	0.55775(2)
***c*(nm)**	1.03363(2)	1.08124(4)	1.05234(3)	1.13298(5)	0.5398(3)	0.61866(9)	0.5934(2)	0.62382(3)	0.55013(1)
c/a	1.962	1.959	1.973	1.998	-	-	-	-	-
Cell volume V(nm^3)	0.28686(4)	0.32948(4)	0.29951(3)	0.36438(5)	0.1653(2)	0.3003(1)	0.2097(2)	0.30962(4)	0.17190(4)
N$^\circ$ atoms in the cell	16	16	16	16	8	16	8	8	8
X-ray density D_x(g/cm^3)	3.96	4.32	4.26	5.66	5.32	3.74	6.09	4.11	5.57
R_{wp}, R_B, R_{exp},	5.19 4.02 2.78	6.23 4.71 3.12	4.04 3.14 2.86	6.26 4.87 3.59	14.9 11.6 8.2	5.02 3.97 2.72	14.4 11.1 10.2	6.97 5.03 2.84	5.98 4.59 3.12
Goodness of fit χ^2	1.87	2.00	1.41	1.74	1.8	1.85	1.4	2.45	1.92
Weight fraction (%)	91.8(4)	99.8(2)	70.4(1)	66.4(7)	40(2)	86.6(5)	73(2)	99.8(2)	74.3(6)
N^o refined parameters	24	23	54	51	68	37	23	47	51
Wavelenght λ(nm)	Cu Kα_1 (0.154059)								
Diffractometer	D8 FOCUS BRUKER								

TABLE II.

Atom	**Ox.**	**Site**	***x***	***y***	***z***	**Foc**	**Biso (Å)**
Cu_2CoSiS_4							
Cu	1+	4d	0.0	0.5	0.25	1.0	1.7(1)
Co	2+	2a	0.0	0.0	0.0	1.0	0.3(2)
Si	4+	2b	0.0	0.0	0.5	1.0	0.5(3)
S	2-	8i	0.2636(4)	0.2636(4)	0.1203(4)	1.0	0.36(9)
Cu_2MnSnS_4							
Cu	1+	4d	0.0	0.50	0.25	1.0	0.94(2)
Mn	2+	2b	0.5	0.5	0.0	1.0	0.67(2)
Sn	4+	2a	0.0	0.0	0.0	1.0	0.52(1)
S	2-	8i	0.2499(5)	0.2499(5)	0.1399(4)	1.0	0.59(2)
Cu_2FeGeS_4							
Cu	1+	4d	0.0	0.50	0.25	1.0	1.22
Fe	2+	2a	0.0	0.0	0.0	1.0	0.88
Ge	4+	2b	0.0	0.0	0.50	1.0	0.42
S	2-	8i	0.265(1)	0.265(1)	0.129(2)	1.0	0.73
$Cu_2CoSnSe_4$							
Cu	1+	4d	0.0	0.5	0.250	1.0	0.5(3)
Co	2+	2a	0.0	0.0	0.0	1.0	1.4(6)
Sn	4+	2b	0.0	0.0	0.5	1.0	1.8(4)
Se	2-	8i	0.2414(4)	0.2414(4)	0.1297(4)	1.0	1.7(2)
$Cu_2CoSiSe_4$							
Cu	1+	4a	0.0	0.0	0.0	0.5	0.3
Co	2+	4a	0.0	0.0	0.0	0.25	0.3
Si	4+	4a	0.0	0.0	0.0	0.25	0.3
Se	2-	4c	0.25	0.25	0.25	1.0	0.6
Cu_2MnSiS_4							
Cu	1+	4b	0.747(3)	0.677(2)	0.166(9)	1.0	1.57(5)
Mn	2+	2a	0.0	0.842(3)	0.667(9)	1.0	1.28(4)

Si	4+	2a	0.0	0.173(6)	0.162(9)	1.0	0.79(4)
S1	2-	2a	0.0	0.856(6)	0.0635	1.0	0.97(4)
S2	2-	4b	0.730(3)	0.663(3)	0.538(6)	1.0	0.96(5)
S3	2-	2a	0.0	0.172(6)	0.496(9)	1.0	0.98(5)
$Cu_2CoGeTe_4$							
Cu	1+	4a	0.0	0.0	0.0	0.5	0.3
Co	2+	4a	0.0	0.0	0.0	0.25	0.3
Ge	4+	4a	0.0	0.0	0.0	0.25	0.3
Te	2-	4c	0.25	0.25	0.25	1.0	0.6
Cu_2MnGeS_4							
Cu	1+	4b	0.248(1)	0.325(1)	0.989(3)	1.0	0.86(2)
Mn	2+	2a	1.00	0.147(2)	0.488(5)	1.0	0.73(5)
Ge	4+	2a	1.00	0.829(1)	0.969(4)	1.0	0.49(4)
S1	2-	2a	1.00	0.795(4)	0.641(6)	1.0	0.59(5)
S2	2-	2a	1.00	0.149(4)	0.107(7)	1.0	0.55(7)
S3	2-	4b	0.264(2)	0.328(3)	0.622(4)	1.0	0.55(7)
$Cu_2CoGeSe_4$							
Cu	1+	4a	0.0	0.0	0.0	0.5	0.3(2)
Co	2+	4a	0.0	0.0	0.0	0.25	0.3(2)
Ge	4+	4a	0.0	0.0	0.0	0.25	0.3(2)
Se	2-	4c	0.25	0.25	0.25	1.0	0.6(1)

TABLE III.

	Cu_2CoSiS_4	**Cu_2MnSnS_4**	**Cu_2FeGeS_4**	**$Cu_2CoSnSe_4$**	**$Cu_2CoSiSe_4$**	**Cu_2MnSiS_4**	**$Cu_2CoGeTe_4$**	**Cu_2MnGeS_4**	**$Cu_2CoGeSe_4$**
Distances									
d_{Cu-X}	0.2297(3)	0.2286(3)	0.228(1)	0.2425(3)	0.2377(3)	0.235(4)	0.2572(2)	0.228(2)	0.24012(1)
						0.231(7)		0.233(2)	
						0.232(3)		0.241(3)	
d_{II-X}	0.2325(3)	0.2470(3)	0.242(1)	0.2431(3)	0.2377(3)	0.245(6)	0.2572(2)	0.248(3)	0.24012(1)
						0.247(3)		0.238(5)	
						0.237(5)		0.248(2)	
d_{IV-X}	0.2156(3)	0.2469(3)	0.223(1)	0.2542(3)	0.2377(3)	0.213(5)	0.2572(2)	0.206(4)	0.24012(1)
						0.217(4)		0.226(3)	
						0.207(8)		0.228(2)	
Angles									
X-Cu-X	108.6(1)	117.2(1)	108.2(4)	111.6(1)	110.8(2)	109.8(2)	109.6(2)	112(1)	110.2(1)
	109.9(1)	105.7(1)	112.0(4)	108.4(1)	109.3(2)	108.2(2)	109.1(2)	109(1)	108.8(1)
						107.8(2)		102(1)	109.3(1)
						114.8(2)		111(1)	
X-II-X	106.6(1)	104.5(1)	111.6(4)	105.6(1)	110.8(2)	109.9(5)	109.6(2)	113(1)	110.2(1)
	115.3(1)	112.0(1)	108.4(4)	111.4(1)	109.3(2)	114.4(5)	109.1(2)	110(1)	108.8(1)
						110.9(5)		108(1)	109.3(1)
						105.9(5)		109(1)	
X-IV-X	109.6(1)	104.4(1)	105.1(4)	109.5(1)	110.8(2)	111.4(2)	109.6(2)	119(1)	110.2(1)
	109.4(1)	112.1(1)	111.7(4)	109.4(1)	109.3(2)	106.4(3)	109.1(2)	112(1)	108.8(1)
						110.8(3)		105(1)	109.3(1)
						106.0(2)		104(1)	

TABLE IV.

N°	Compound	a_e (Å)	E_h (eV) Observed	E_h (eV) Predicted	C_i (eV) Observed	C_i (eV) Predicted	f_i (eV) Observed	f_i (eV) Predicted	Ref.
1	Cu_2MnSiS_4	5.3152	5.00	4.86	6.01	5.97	0.59	0.59	Our
2	Cu_2MnGeS_4	5.3661	4.84	4.74	5.91	5.96	0.60	0.60	Our
3	$Cu_2MnSn\ S_4$	5.4796	4.47	4.45	5.92	5.88	0.64	0.63	Our
4	$Cu_2FeGe\ S_4$	5.3111	4.96	4.87	6.20	6.09	0.61	0.60	Our
5	$Cu_2CoSi\ S_4$	5.2345	5.25	5.12	6.39	6.24	0.60	0.59	Our
6	$Cu_2CoSiSe_4$	5.4886	4.65	4.37	5.96	5.21	0.62	0.56	Our
7	$Cu_2CoGeSe_4$	5.5507	4.53	4.26	5.83	5.21	0.62	0.57	Our
8	$Cu_2CoSnSe_4$	5.6689	4.23	4.04	5.62	5.21	0.64	0.60	Our
9	$Cu_2CoGeTe_4$	5.9411	3.81	3.57	4.99	4.37	0.63	0.57	Our
10	Cu_2CoGeS_4	5.2761	5.04	4.98	6.46	6.20	0.62	0.60	[7]
11	Cu_2CoSnS_4	5.4025	4.74	4.45	6.28	5.78	0.64	0.60	[7]
12	$Cu_2MnSnSe_4$	5.7361	4.15	3.92	5.49	5.09	0.64	0.60	[20]
13	$Cu_2FeSnSe_4$	5.6820	4.20	3.92	5.58	5.03	0.64	0.59	[16]
14	$Cu_2ZnGeSe_4$	5.5798	4.47	3.98	5.68	4.81	0.62	0.54	[18]
15	$Cu_2CdSnSe_4$	5.7867	3.92	3.99	5.11	5.27	0.63	0.64	[19]

4. Conclusion

The results showed that Cu_2MnSnS_4, Cu_2FeGeS_4, Cu_2CoSiS_4 and $Cu_2CoSnSe_4$ have a tetragonal stannite structure with space group $I\bar{4}2m$(N° 121), Cu_2MnSiS_4 and Cu_2MnGeS_4 an orthorhombic wurtz-stannite structure with space group $Pmn2_1$(N° 31), $Cu_2CoSiSe_4$, $Cu_2CoGeSe_4$ and $Cu_2CoGeTe_4$ an orthorhombic pseudo-cubic structure with space group F222 (N° 22). It was found that the values of the atomic positions (Δx and Δz), the tetragonal distortion (δ) and the internal distortion (σ) versus W for compounds containing S and/or Se lay on different lines, this behavior was correlated with the large difference between the atomic weight of the S and Se anions. Also, it appeared that, independent of the crystal structure and kind of anion involved, for each case, the experimental points of $d_{\text{Cu - VI}}$, $d_{\text{II - VI}}$ and $d_{\text{IV - VI}}$ vary linearly with the parameter a_e. It was found that the resulting observed and predicted values of C_i are similar; identical results were obtained for the observed and predicted values of E_h. Also, it was found that the resulting observed and the predicted values of C_i and E_h lie on the same straight line, independently of the type of anion involved and crystal structure. Thus, the values of C_i and E_h, for a given tetrahedrally coordinated crystal with effective lattice parameter a_e, can be predicted based only on their constituent atomic properties data. It was observed that the values of C_i and E_h vary linearly with the effective parameter a_e.

Acknowledgments

This work was partially supported by the CDCHT-ULA (Project No. C-1740-11-05-AA). E. Moreno would like to thank the Plan de Desarrollo de Talentos Humanos de Alto Nivel of FONACIT, through contract No. 200601411, Venezuela. S. Alvares would like to thank the Plan de Desarrollo de Talentos Humanos de Alto Nivel of FONACIT, through contract No. 200801535, Venezuela. P. Grima-Gallardo would like to thank to FONACIT, project PEII No 1697. M. A. Macías would to thank COLCIENCIAS (Colombia) for his doctoral fellowship. The authors would like to thank to the reviewer for its interest in this work and critical reading of the manuscript.

1. H. Katagiri, K. Jimbo, W. S. Maw, K. Oishi, M. Yamazaki, H. Araki and A. Takeuchi, *Thin Solid Films*, **517** (2009) 2455–2460.
2. Y. Shapira, E.J. McNiff Jr., N.F. Oliveira Jr., E.D. Honig, K. Dwight and A. Wold, *Phys. Rev. B*, **37** (1988) 411.
3. L. Guen and W. S. Glaunsinger, *J. Sol. Stat. Chem.*, **35** (1980) 10.
4. X. L. Chen, A. M. Lamarche, G. Lamarche, and J. C. Woolley, *J. Magn. Magn. Mater.* **118** (1993) 119.
5. E. Quintero *et al*., *J. Phys. Chem. Solids*, **71** (2010) 993.
6. W. Schäfer and R. Nitsche, *Mat. Res. Bull.* **9** (1974) 645.
7. L. D. Gulay, O. P. Nazarchuk and I. D. Olekseyuk, *J. Alloy Compd.* **377** (2004) 306.

8. M. Quintero *et al*., *Mater. Res. Bull.* **34** (1999) 2263-2270.
9. E. Parthé, K. Yvon, and R. H. Deitch, *Acta Cryst.,* **B25** (1969) 1164.
10. A.-M. Lamarche, A. Willsher, L. Chen, G. Lamarche and J.C. Woolley, *J. Sol. Stat. Chem.*, **94** (1991) 313-318.
11. A. Boultif and D. Loüer. *J. Appl. Cryst.* **37** (2006) 724.
12. LMGP-Suite Suite of Programs for the interpretation of X-ray Experiments, by Jean laugier and Bernard Bochu, ENSP/Laboratoire des Matériaux et du Génie Physique, BP 46. 38042 Saint Martin d'Hères, France. WWW: http://www.inpg.fr/LMGP and http://www.ccp14.ac.uk/tutorial/lmgp/.
13. A. D. Mighell, C. R. Hubbard, and J. K. Stalick, *NBS*AIDS83: A Fortran Program for Crystallographic Data Evaluation, National Bureau of standards* (USA), Tech note 1141, (1981).
14. Lutterotti L. Material Analysis using Diffraction - MAUD: Computer code JAVA. Trento: University of Trento. 1997-2009. Available from: http://www.ing.unitn.it/∼maud/.
15. R. A. Young, *Editor. The Rietveld Method*. (Oxford University Press, Oxford, 1993).
16. J. A. Henao *et al*., *Chalcogenide Lett.* **6** (2009) 583.
17. O. V. Parasyuk, L. D. Gulay, Ya. E. Romanyuk, and L. V. Piskach, *J. Alloy Compd.*, **329** (2001) 202.
18. V. P. Sachanyuk, I. D. Olekseyuk, and O. V. Parasyuk, *phys. stat. sol. (a)* **203** (2006) 459.
19. I. D. Olekseyuk, L. D. Gulay, I. V. Dydchak, L. V. Piskach, O. V. Parasyuk, and O. V. Marchuk, *J. Alloy Compd.* **340** (2002) 141.
20. J. A. Van Vechten and T. K. Bergstresser, *Phys. Rev.* **1** (1970) 3351.
21. J. C. Phillips, *Rev. Mod. Phys.* **42** (1970) 317.
22. B. Cordero *et al*., *Dalton Trans.*, (2008) 2832.